

A HYBRID METHOD TO SIMULATE AN INDUCTIVELY COUPLED AR-HG PLASMA

^{1,2}YANG LIU, ³GEORGES ZISSIS, ^{1,2,*}YUMING CHEN

¹Institute for Electric Light Sources, Fudan University; 220 Handan Road, Shanghai 200433, China

²Engineering Research Center of Advanced Lighting Technology, Ministry of Education, 220 Handan Road, Shanghai 200433, China

³LAPLACE (Laboratoire Plasma et Conversion d'Energie) Universite Paul Sabatier - Toulouse III Build. 3R2; 118 rte de Narbonne F-31062 Toulouse Cedex 9; FRANCE

Email: ly@fudan.edu.cn, georges.zissis@laplace.univ-tlse.fr, yumingchen@fudan.edu.cn

ABSTRACT

A hybrid method is used in simulating an inductively coupled Ar-Hg discharge plasma. In this hybrid model the combination of plasma fluid model and the Boltzmann Equation is applied. With this model, not only the “macroscopic” parameters of the discharge, such as electron density, electron temperature, can be simulated, but also the electron behavior can be derived, which is not accessible in mere fluid model.

Keywords: *Inductively Coupled Plasma, Ar-Hg Discharge, Electrodeless Fluorescent Lamp, Fluid Model, Boltzmann Equation, Hybrid Method*

1. INTRODUCTION

In the past twenties, electrodeless fluorescent lamps based on inductively coupled Ar-Hg discharge become known to the public due to its longevity and high efficacy. Scientists made efforts from different aspects to clarify mechanisms behind the discharge plasma. In theoretical sense, plasma models were established to reveal the physics difficult to be found in experiments [1 - 9]. But efforts are still needed for better and deeper understanding of the discharge. In plasma fluid model, rate coefficients are important input parameters because they can significantly affect simulation results. To calculate rate coefficients, electron energy distribution function (EEDF) must be known. For simplicity, previous models usually assumed a Maxwellian EEDF [9, 10]. In high current and high frequency discharge, this assumption is mostly justified. But detailed description on electron behavior is missing in this case. To overcome this fault, it would be best to directly solve the Boltzmann Equation of electron. But the colossal mathematical efforts behind hinder the pathway. Now, two major comprising methods are present. One is to combine particle-in-cell (PIC) model and fluid model; the other is to combine energy-domain Boltzmann Equation and fluid model. In this article, we will simulate an inductively coupled plasma by combination of plasma fluid model and the Boltzmann Equation.

With this model, we can have information on “macroscopic” parameters of the discharge, such as electron density, electron temperature and so on; furthermore, we can also have description on electron behavior, which is not accessible in mere fluid model. The remaining part of this article is organized as follow: in Section 2, the subject discharge will be introduced; in Section 3, model composition will be explained; in Section 4, solution method of the model is presented, in Section 5, some of the simulation results will be given and in Section 6, summary of the paper will be made.

2. DISCHARGE DESCRIPTION

Fig. 1 shows the structure and dimension of the subject discharge bulb. The bulb has the similar shape as the Philips QL lamp, where the upper part is spherical and the lower part is cylindrical. The bulb has a re-entry chamber in the center to allow insertion of ferrite core and coil. Once electricity is on, discharge will be induced on the azimuthal direction (shown by the arrow in Fig. 1). Since the bulb is spherically symmetric, simulation will be performed only in the painted region of Fig. 1. Dimension of the discharge chamber has already been annotated on Fig. 1.

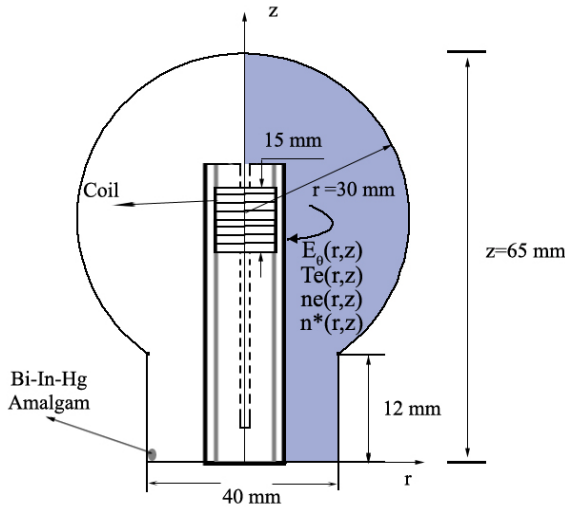


Fig. 1 Structure And Dimension Of The Subject Discharge Bulb

3. MODEL INTRODUCTION

The model consists of three parts: the electro-magnetic part, the plasma fluid part, and the Boltzmann Equation part.

3.1 Electro-magnetic part

The discharge is excited by high frequency electric-magnetic field (2.65 MHz). Variation of electro-magnetic field is governed by the Maxwell Equations. Taking into account cylindrical symmetry and omitting displacement current, azimuthal electric field $E_{\theta}(r,z)$ can be written as:

$$\nabla^2 E_{\theta}(r, z) = \mu_0 \frac{\partial}{\partial t} (\sigma E_{\theta}(r, z)) \quad (1)$$

where ϵ is permittivity, and σ is conductivity. Conductivity under high frequency can be expressed as:

$$\sigma = -n_e e \frac{E}{3} \sqrt{\frac{2e}{m_e}} \int_0^{\infty} \epsilon \frac{v_m - i\omega}{v_m^2 + \omega^2} \frac{\partial f}{\partial \epsilon} d\epsilon \quad (2)$$

where n_e is electron density, e is Coulomb charge, m_e is electron mass, v_m is momentum transfer frequency, ω is angular frequency of electric field, ϵ is electron kinetic energy, and f is EEDF. Electron density is an important parameter, and it may influence production and loss of excited atoms, energy transportation in the space, and so on. This will be addressed in the plasma part of the model. Thus, electron density bridges the electro-magnetic part and the plasma fluid part. The EEDF is governed by the Boltzmann Equation part. Once

the EEDF changes, conductivity may also follow suit. Therefore, the electro-magnetic part and the Boltzmann Equation part are also linked together.

3.2 Plasma fluid model part

The plasma fluid model is the central part of the simulation. The governing equation of this part is the Navier-Stokes equation. In the model, we consider variation of Ar metastable state, Hg $6^{-3}P_{0,1,2}$, Hg $6^{-1}P_1$, Hg $7^{-3}S_1$ and Hg 6-D states. The metastable state Ar and Hg 6-D states are actually combination of several close states by the method introduced in [11]. Besides, electron density, electron temperature, and gas temperature are also calculated. Therefore, the equation system of the plasma fluid part has 10 variables as follows: electron density n_e , electron temperature T_e , metastable Ar atom n_{ArMe} , Hg $6^{-3}P_0$ state atoms n_{3P0} , Hg $6^{-3}P_1$ state atoms n_{3P1} , Hg $6^{-3}P_2$ state atoms n_{3P2} , Hg $6^{-1}P_1$ state atoms n_{1P1} , Hg $7^{-3}S_1$ state atoms n_{3S1} , Hg 6-D state atoms n_{6D} , and gas temperature T_{gas} .

The governing equation of electron density n_e is shown in Eq. 3

$$\frac{\partial n_e}{\partial t} + \nabla \cdot (-D \nabla n_e) = R \quad (3)$$

where D is diffusion coefficient of electrons, R is sum of electron production and loss involved in all kinds of plasma reactions. In the model, we consider radial transportation of electrons is dominated by ambipolar diffusion, i.e.

$$D \approx \mu_i T_e \quad (4)$$

Detailed processes of obtaining Eq. 4 can be retrieved in [9] and [10].

The governing equation of electron temperature T_e is shown in Eq. 5.

$$1.5 \frac{\partial n_e T_e}{\partial t} + 2.5 \nabla \cdot (-n_e D \nabla T_e) = P_{Heating} - P_{Loss} \quad (5)$$

where $P_{Heating}$ is ohm heating by electric field; P_{Loss} is energy loss of electrons by collision; and D is the ambipolar diffusion coefficient. According to [12], ohm heating can be calculated with

$$P_{Heating} = \frac{1}{2} \sigma_r |E_{\theta}|^2 \quad (6)$$

where

σ_r is the real part of conductivity

Gas temperature of the plasma T_{gas} can be obtained with

$$1.5 \frac{\partial n_{Ar} T_{gas}}{\partial t} + 2.5 \nabla \cdot (-n_{Ar} D_{gas} \nabla T_{gas}) = P_{gas_heating} \quad (7)$$

where n_{Ar} is density of ground state Ar atoms, D_{gas} is diffusion coefficient of the gas, and $P_{gas_heating}$ is the source of heating. Since Ar atom is far more than that of Hg in the bulb, T_{gas} can be taken as the temperature of Ar gas. Therefore, we use Ar diffusion coefficient as D_{gas} . Assume that Ar ion and Ar atom diffuse at the same velocity, and follow the Einstein relation, we

have $D_{gas} = D_{Ar} = \frac{kT_{gas}}{e} \mu_{Ar}$, where k is the

Boltzmann constant, μ_{Ar} is ion mobility of Ar, i.e. $0.134 \text{ m}^2 \text{ V}^{-1} \text{ s}$. Major channel of gas heating is elastic collision between electrons and ground state Ar atoms.

The governing equation of all excited atoms can be expressed as:

$$\frac{\partial n^*}{\partial t} + \nabla \cdot (-D_{n^*} \nabla n^*) = R_{n^*} \quad (8)$$

where D_{n^*} is diffusion coefficient of excited atoms, R_{n^*} is the sum of production and loss of excited atoms.

In the model, production and loss of electrons, and excited atoms are incurred in various plasma reactions. We consider miscellaneous plasma reactions caused by electron collision such as excitation and deexcitation, direct ionization, and stepwise ionization. Also, we consider reactions between atoms, such as Penning ionization and so on. Detailed information on reaction types and cross sections can be found in Section 3.2 in [9].

3.3 Boltzmann Equation part

The Boltzmann Equation is

$$\frac{\partial f}{\partial t} + \vec{v} \cdot \nabla_r f - \frac{e}{m} \vec{E} \cdot \nabla_v f = C^{el}(f) + \sum_k C_k^{in}(f) \quad (9)$$

where f is EEDF, E is electric field, v is electron velocity, ∇_r is space gradient, ∇_v is gradient in velocity space, C^{el} is elastic collision term, and C_k^{in}

is non-elastic collision term. Using the two-term expansion, replacing velocity v with kinetic energy u , and omitting space variation, we can finally get the energy domain Boltzmann Equation:

$$\begin{aligned} & \frac{E}{3} \frac{\partial}{\partial u} \left(u \frac{E}{N \sigma_m} \frac{\partial F_0}{\partial u} \right) + 2 \frac{m}{M} \frac{\partial}{\partial u} (N \sigma_m u^2 F_0) \\ & = N \sum_k [F_0(u) u \sigma_{ex}^k(u) - F_0(u + V_{ex}^k)(u + V_{ex}^k) \sigma_{ex}^k(u + V_{ex}^k)] \\ & + N \sum_k [F_0(u) u \sigma_{io}^k(u) - 2F_0(2u + V_{io}^k)(2u + V_{io}^k) \sigma_{io}^k(2u + V_{io}^k)] + \frac{\partial F_0}{\partial t} \Big|_{ee} \end{aligned} \quad (10)$$

where F_0 is isotropic part of EEDF ($\int_0^\infty F_0(u) u^{0.5} du = 1$), N is atom density, σ_m is momentum transfer cross section, M is mass of atom, σ_{ex}^k is excitation cross section of species k , V_{ex}^k is excitation energy of species k , σ_{io}^k is ionization cross section of species k , V_{io}^k is ionization energy of species k , and $\frac{\partial F_0}{\partial t} \Big|_{ee}$ are terms

for electron-electron collision. Mathematical details of obtaining Eq. 10 can be retrieved in [13] and [14].

In the present case, the discharge is run by rf power, therefore, the first term of Eq. 10 becomes

$$\frac{1}{2} \frac{E}{3} \frac{\partial}{\partial u} \left[\frac{(N \sigma_m)^2 u E}{(N \sigma_m)^2 + (m^2 \omega / 2eu)} \frac{\partial F_0}{\partial u} \right] \quad (11)$$

where

$1/2$ comes from the time average of electric field.

3.4 Coupling of different parts of the model

Fig. 2 shows the internal linking between different parts of the model. The electro-magnetic part provide the other two parts information of electric field. It receives information of electron density n_e and EEDF for next round of calculation. The plasma fluid model part obtains rate coefficients from the Boltzmann Equation part plus the electric field. Then it outputs atom densities of different species and electron density n_e . While the Boltzmann Equation part receives electric field and atom densities, and gives EEDF and rate coefficients. The calculation starts from some trial results. As long as the trial is in reasonable range, calculation will always converge to some certain results. The three parts form a self-consistent system, and the input parameters such as gas species, gas pressure, collision cross sections etc define features of the system, and finally decide what results will be gotten.

\square is angular frequency

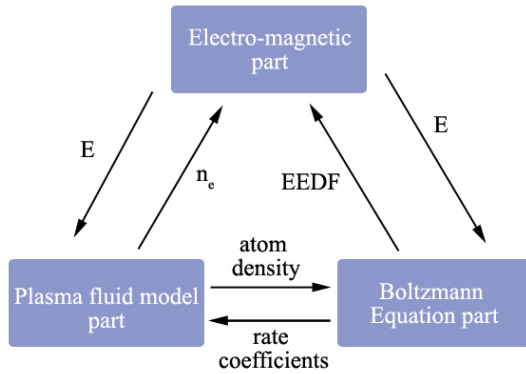


Fig. 2 Inner Correlation Between Different Parts Of The Model

4. MODEL SOLUTION

Fig. 3 depicts the solution area of the model. The Maxwell equations and fluid equations are solved with finite element method. The mesh grid is also shown in Fig. 3. The Boltzmann Equation (Eq. 10) can be solved with finite difference method (as in [13]) or finite volume method (as in [14]). In the present model, we use finite volume method with uniform mesh grid. EEDF is obtained as function of electric field E and electron density n_e . Then rate coefficients are calculated and formed as interpolation tables. The plasma fluid model may find necessary rate coefficients by inputting E and n_e values into the table.

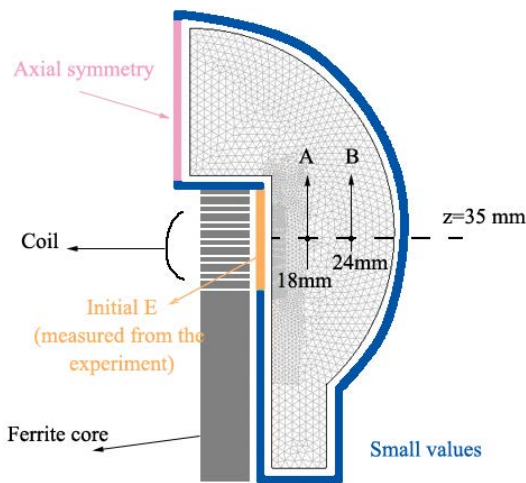


Fig. 3 Solution Area And Boundaries

For electro-magnetic part, boundary conditions are such that near the coil, electric field equals local potential divided by coil perimeter; at the upper leftmost boundary, axial symmetry is assumed; and at all other boundaries, electric field equals zero. The local potential near the coil can be obtained from experiment with single coil method. Detail

information on this can be found in [15]. In the present case, the boundary E there is 202.2 V/m. For plasma fluid model part, we consider there is no discharge on the boundary. So except that the upper leftmost boundary is axial symmetry, boundary particle density, electron temperature, and gas temperature are set to very small values.

Choice of initial values of electric field, particle densities, electron temperature, and gas temperature is somewhat free. As long as initial values are in a proper range, simulation will always converge to a certain point, which is mainly determined by intrinsic properties of the model defined gas type, gas filling pressure, and collision cross sections and so on.

5. RESULTS

Fig. 4 shows the calculated electron density n_e and Hg 6^3P_1 atom density. From the figure we can see that the maximum value of electron density locate near the coil; while the Hg 6^3P_1 atom are more widely spread in the discharge space. Fig. 5 presents the calculated EEDF on point A and B shown in Fig. 3. It can be seen that when kinetic energy is below 7eV, the two EEDFs almost coincide. That means electron behavior in both cases is similar. Differences start to become significant when kinetic energy is beyond 7eV. Due to smaller distance from the coil, the EEDF of point A reveals higher percentage of fast electrons. Therefore, we can expect that excitation and ionization are much stronger here than at point B, which explains why electron density is higher in region close to the coil.

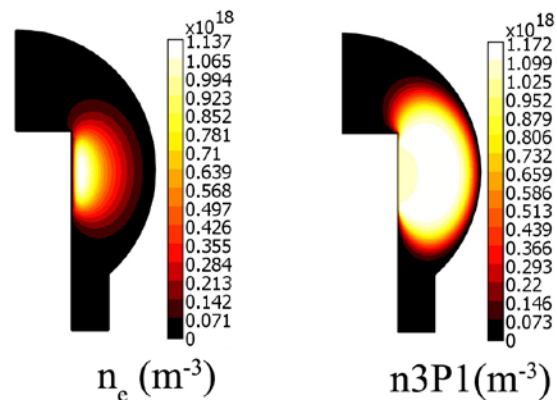


Fig. 4 Calculated Electron Density N_e And Hg 6^3P_1 Atom Density

The hybrid method used in this article is superior over mere plasma fluid model in the sense that the hybrid model can provide extra information. For plasma fluid model, it is often assumed that the EEDF is Maxwellian. In most cases, this

assumption can be justified, and simulation results can be credible. Nevertheless, this assumption may not reflect variation in electron behavior properly, because variation in EEDF is already defined by the Maxwell distribution function for a Maxwellian EEDF. It means that behavior of electrons with different velocity has already been prescribed. This is obviously not necessarily the case since we cannot know exactly how electrons will behave beforehand. In this hybrid model, no prescription on electron behavior is made. The EEDFs are obtained by directly solving the Boltzmann Equation. Therefore, we can have more detailed analyses on the discharge. For a Maxwellian EEDF, one set of rate coefficients corresponds to only one fixed distribution of EEDF. In a hybrid model, one set of rate coefficients may correspond to several different EEDFs since distribution of EEDF may vary. This allows us to know more details of the discharge.

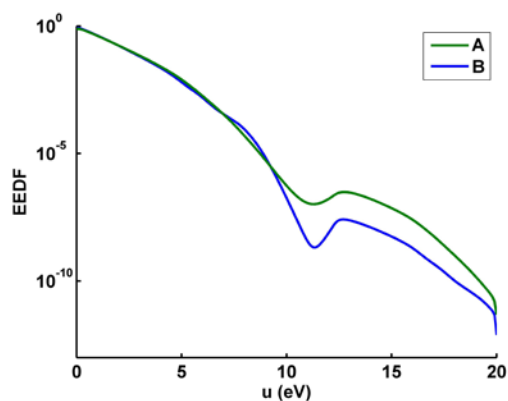


Fig. 5 EEDF At Two Different Points Of The Discharge

6. SUMMARY

In this article, simulation of an inductively coupled Ar-Hg plasma is performed with a hybrid method. The model consists of three parts: electromagnetic part, plasma fluid part, and Boltzmann Equation part. These three parts form a self-consistent system. Not only can the model provides information on plasma parameters such as electron density, excited atom densities, and so on; it can also reflect electron behavior since EEDF can be obtained in the Boltzmann Equation part. That makes the method stronger than mere plasma fluid model. Such simulation may become a powerful tool for discharge design.

REFERENCES

- [1] J. W. Denneman, J. Phys. D: Appl. Phys. **23** 293 (1990)
- [2] G. G. Lister and M Cox, Plasma Sources Sci. Technol. **1** 67 (1992)
- [3] Eugen Statnic and Valentin Tanach, Plasma Sources Sci. Technol. **13** 515 (2004)
- [4] Eugen Statnic and Valentin Tanach, Plasma Sources Sci. Technol. **15** 465 (2006)
- [5] Kapil Rajaraman and Mark J Kushner, J. Phys. D: Appl. Phys. **37** (2004) 1780–1791
- [6] J. J. Curry G. G. Lister and J. E. Lawler, J. Phys. D: Appl. Phys. **35** 2945 (2002)
- [7] N. Denisova, G. Revalde and A. Skudra, J. Phys. D: Appl. Phys. **38** 3269 (2005)
- [8] N. Denisova, G. Revalde, A. Skudra, G. Zissis and N. Zorina, J. Phys. D: Appl. Phys. **38** 3275 (2005)
- [9] Yang Liu, Georges Zissis and Yuming Chen, Journal of Physics D: Applied Physics **44** (2011) 305201
- [10] Ka Hong Loo et al, IEEE Transactions On Power Electronics **19** (4) 1117 (2004)
- [11] Bogaerts A. and Gijbels R. et al. J. Appl. Phys. **84** 121 (1998)
- [12] P. Scheubert, P. Awakowicz, R. Schwefel, G. Wachutka, Surface and Coatings Technology **142-144** 526 (2001)
- [13] G. J. M. Hagelaar et al. Plasma Sources Sci. Technol. **14** 722 (2005)
- [14] Dyatko N A, Kochetov I V, Napartovich A P, Sov. J. Plasma Phys. **18** (7), 462 (1992)
- [15] W. P. Li, Y. Liu et al. Journal of Applied Physics **104** 083306 (2008)